ELSEVIER

Polymer 42 (2001) 6699–6708

polymer

www.elsevier.nl/locate/polymer

Thermoplastic elastomers 1. Poly(ether-ester-imide)s based on 1,4-diaminobutane, trimellitic anhydride, 1,4-dihydroxybutane and poly(tetramethylene oxide) diols

Hans R. Kricheldorf[a,*], Thomas Wollheim[a], Cor E. Koning[b], H. Gerard Werumeus-Buning[b], Volker Altstädt[c]

[a]*Institut für Technische und Makromolekulare Chemie, Bundesstr. 45, D-20146 Hamburg, Germany*
[b]*DSM Research, Section EP-CP, P.O. Box 18, NL-6160 MD Geleen, Germany*
[c]*TU-Hamburg-Harburg, Denickestr. 15, D-21073 Hamburg, Germany*

Received 4 October 2000; received in revised form 6 February 2001; accepted 17 February 2001

Abstract

Starting from 1,4-diaminobutane and trimellitic anhydride a bisimide dicarboxylic acid was prepared which was transformed into its diethyl ester. This imide monomer was polycondensed with mixtures of 1,4-dihydroxybutane and poly(tetramethylene oxide) (PTMO) diols having number average molecular weights (M_ns) of 650, 1000 or 2000 Da. For each PTMO diol, the weight fraction of the hard segments was varied from 30 over 40 and 50–60%. For the PTMO diols 1000 and 2000, macrophase separation was observed during polycondensation. This problem was solved in the case of PTMO-1000 by a PTMO diol of greater polydispersity. The chemical structure of the poly(ether-ester-imide)s, PEEIs, was characterized by IR and ^{1}H NMR spectroscopy. The phase transitions were identified by DSC and DMTA measurements, which revealed that all members of this series were slowly crystallizing materials. The mechanical properties were determined by stress–strain and hysteresis measurements. Macrophase separation during the polycondensation was reflected in poorer mechanical properties.

Keywords: Thermoplastic elastomers; Polyimides; Poly(tetramethylene oxide)

1. Introduction

Thermoplastic elastomers (TPEs) combine two interesting and useful properties, namely an elasticity comparable to that of covalently crosslinked rubbers and a meltability allowing for processing from the melt (e.g. by extrusion or injection molding) quite analogous to normal engineering plastics. TPEs may be described as multiblock copolymers consisting of rapidly crystallizing hard segments and amorphous or low melting soft segments having a glass transition temperature (T_g) below −20 or better below −40°C. The technically produced TPEs possess hard segments generally based on oligourethanes or on aromatic polyesters and soft segments derived from aliphatic polyesters or from aliphatic polyethers. The polyethers are more frequently used, because they are stable against hydrolysis and transesterification and because they possess lower T_gs.

The first studies of poly(ether-ester) TPEs were reported by Coleman [1,2] immediately followed by work of Charch and Shrivers [3,4]. These authors used the slowly crystallizing poly(ethylene terephthalate), PET, hard segments. The most successful combination, the rapidly crystallizing poly(butylene terephthalate), PBT, in combination with PTMO soft segments (see structure of PEE **1**) was first described by Nishimura and Komogata [5] and later studied in more detail by Witsiepe [6–8]. Recent reviews summarize the further development of TPEs based on poly(ether-ester)s [9–11].

A disadvantage of the commercial poly(ether-ester)s is a partial compatibility of the hard segments and the soft segments. Even an only poor compatibility reduces the crystallinity and mechanical stability of the hard phase and raises the T_g of the soft phase. In this connection, hard segments containing imide building blocks were of interest, because the high polarity and planarity of aromatic imide groups should favor the microphase separation and possibly a rapid crystallization. The present work is the first part of a broader study of TPEs containing imide units in the hard segments.

* Corresponding author.
E-mail address: kricheld@chemie.uni-hamburg.de (H.R. Kricheldorf).

0032-3861/01/$ - see front matter
PII: S0032-3861(01)00151-3

Compared to commercial PBT based TPEs the poly(ether-ester-imide)s (PEEIs) of this work should contain a bisimide dicarboxylic acid replacing the terephthalic acid. In other words, the PEEIs **2**, **3** and **4** should be synthesized and characterized.

2. Experimental

2.1. Materials

Trimellitic anhydride, 1,4-diaminobutane, 1,4-dihydroxybutane and dimethyl terephthalate were purchased from Aldrich Co. (Milwaukee, WI, USA). The poly(tetramethylene oxide) diols, PTMO-650, -1000 and -2000, were gifts of DSM Research. These PTMO samples were products of BASF AG. Furthermore, an additional PTMO-1000 of Mitsubishi Chem.Co. was used. All diols were azeotropically dried with toluene and the 1,4-dihydroxybutane was then distilled in vacuo. The dimethyl formamide (DMF) was distilled over P_4O_{10} in vacuo. The antioxidant Irganox 1330® was also a gift of DSM Research.

2.2. Bisimide diethyl ester *6*

(A) Bisimide dicarboxylic acid **5.** 1,4 Diaminobutane (0.4 mol) and trimellitic anhydride (0.82 mol) were dissolved in dry DMF (600 ml) and stirred for 2 h at 100°C. Acetic anhydride (1.0 mol) was then added dropwise and the temperature was raised to 120°C for 2 h. After cooling, the reaction mixture was poured into cold water, the crystallized product was filtered off, washed with water, dried at 60°C in vacuo and recrystallized from DMF. Yield: 75%, mp: 355–357°C (DSC, mp 343–345°C in Ref. [12]).

(B) The bisimide dicarboxylic acid **5** (0.3 mol) was refluxed in distilled thionylchloride (400 ml) and a solution of DMF (1 ml) in chloroform (10 ml) was added dropwise over a period of 8 h. The reaction mixture was refluxed for additional 8 h and finally concentrated in vacuo. Toluene (200 ml) was added to the residue and evaporated in vacuo. This process was repeated to remove remaining thionylchloride. The crude product was then dispersed in dry ethanol (600 ml), dry pyridine (20 ml) was added and this mixture was refluxed for 48 h. The product, which had precipitated after cooling with ice, was filtered off, and recrystallized from DMF: Yield: 86%, mp: 186–187°C. Analyses calcd for $C_{26}H_{24}O_8N_2$ (492.5): C 63.41, H. 4.91, N 5.69, found: C 63.39, H 4.88, N 5.76%. ^{1}H NMR ($CDCl_3$/TMS): $\delta = 1.43$ (t, 6H), 1.69 (mc, 2H), 3.70 (t, 2H) 4.43 (q, 4H),7.90 (d, 4H), 8.41 (mc, 8H), 8.47 (s, 2H) ppm.

2.3. Polycondensations

2.3.1. PEEI *2a*

The bisimide diethyl ester **6** (10.2 mmol), 1,4-dihydroxybutane (15.3 mmol), PTMO-650 (5.33 mmol), 40 mg Irganox® 1330, and 250 mg of a solution containing 4 g of $Ti(OBu)_4$ in 1 l of 1,4-dihydroxybutane were weighed into a cylindrical glass reactor. This reactor was equipped with gas-inlet and -outlet tubes and with a metal stirrer. The reaction vessel was placed into an oil bath preheated to 100–120°C and the temperature was rapidly raised to 195°C. After 1 h, the temperature was raised successively to 210°C for 1 h, 220°C for 1 h and then to 250°C for 2.5 h. During the last heating phase, vacuum was applied to remove excess diol and drive the polymerization to completion. Finally the hot melt was removed mechanically from the reactor and cooled with cold water. The isolated PEEIs were dried at 60°C in vacuo. Purification by dissolution and precipitation was not applied to avoid degradation of the PTMO blocks by residual acidic (co)solvents (e.g. trifluoroacetic acid or formic acid) and to avoid the residual solvent that affects the mechanical properties.

2.3.2. PEE *1*

Dimethyl terephthalate (119.75 g, 617 mmol), 1,4-dihydroxybutane (83.4 g, 925 mmol), PTMO-1000 (92.4 g, 92.4 mmol), Irganox® 1330 (1.1 g) and 3.0 g of a solution containing 4.0 g of $Ti(OBu)_4$ in 1 l of 1,4-dihydroxybutane were weighed into an 1 l stainless steel reactor equipped with a mechanical stirrer. The reaction mixture was heated to 200°C over a period of 1 h, whereby the liberated methanol was removed with a slow stream of nitrogen. The temperature was then raised to 225°C and a vacuum of 12–15 mbar was applied. After 40 min, the temperature was raised to 240°C and a vacuum of 1.5 mbar was applied. The reaction was stopped 2.5 h later, and the polyester was extruded under pressure into cold water. The isolated poly(ether-ester) was dried at 60°C in a vacuum of 12 mbar. Because of losses resulting from the mechanical work-up procedure no yields were determined.

2.4. Measurements

The inherent viscosities were measured with an automated Ubbelohde viscometer thermostated at 25°C with solutions containing 1 g PEEI in 1 l of azeotropically dried *m*-cresol. The DSC measurements were performed on a Perkin–Elmer DSC-7 in aluminum pans under nitrogen with a heating rate of 20°C/min. The mp of the monomer was determined at a heating rate of 3°C/min.

The IR spectra were recorded with KBr pellets on a Nicolet Md "Impact 410" FT IR-spectrometer. The ^{1}H NMR spectra were recorded with a Bruker AMX 400 FT NMR spectrometer in 5 mm o.d. sample tubes. $CDCl_3$ or a mixture of $CDCl_3$ and trifluoroacetic acid (volume ratio 4:1) containing TMS as internal shift reference served as solvent.

The wide angle X-ray measurements were conducted with a Siemens D-500 diffractometer using Ni-filtered CuK_α radiation at 25°C. Films having a thickness of 0.5 mm were melt-pressed and annealed for this purpose.

Table 1
Composition and properties of the PEEIs **2**, **3, 4** and PEE **1**

Polymer	Hard segment (wt%)[a]	PTMO (weight%)[a]	η_{inh}[b] (dl/g)	T_m (°C)	
				1. heat	2. heat
PEEI **2a**	30	43.2	0.46	188	193
PEEI **2b**	40	37.0	0.81	207	208
PEEI **2c**	50	30.8	0.60	219	222
PEEI **2d**	60	24.7	0.73	241	241
PEEI **3a**	30	49.9	1.23	192	209
PEEI **3b**[c]	40	42.8	1.25	209	217
PEEI **3b**′[d]	40	42.8	1.25	209	219
PEEI **3c**	50	35.6	0.78	224	227
PEEI **3d**	60	28.5	1.02	236	237
PEEI **4a**	30	58.3	1.17	20,238	24,240
PEEI **4b**	40	49.9	1.13	20,241	25,243
PEEI **4c**	50	41.6	0.80	21,243	23,245
PEEI **4d**	60	33.3	1.33	23,246	27,248
PEE **1**	52.4	42.0	1.39	194	196

[a] The imide units covalently bound to the PTMO segments and belonging tothe soft segments (see formulas **2**, **3** and **4**) represent the difference to 100%.
[b] Measured at 25°C with $c = 1$ g/l in *m*-cresol.
[c] A PTMO-1000 of BASF AG having a polydispersity of 1.9 was used.
[d] A PTMO-1000 of Mitsubishi Chemical Corporation having a polydispersity of 2.2 was used.

The DMTA measurements were performed on a Rheometrics RSA-II apparatus using annealed melt-pressed films. A frequency of 1 Hz and a heating rate of 3°C/min (starting a −130°C) were used for all measurements.

For the stress–strain measurements S 3A tensile specimens (DIN 53544) were prepared from films having a thickness of 0.5 mm. The measurements were conducted at a constant draw rate of 50 mm/min on a Zwick Md 1445 apparatus and evaluated with the Zwick software 7005. Each value represents an average of five measurements. For the hysteresis measurements, the same apparatus in combination with the 7007 software was used. The measurements were conducted at 20°C with 10 cycles applying a strain of 100 or 500% and a draw ratio of 10 mm/min. Each value represents an average of three measurements.

3. Results and discussion

3.1. Syntheses

In order to allow a comparison of the new PEEIs **2**–**4** with a standard TPE the poly(ether-ester) PEE **1** was prepared from PTMO-1000, 1,4-dihydroxybutane and dimethyl terephthalate. This academic TPE was used as standard instead of a commercial sample for three reasons: firstly, contamination with additives should be avoided; secondly, the PTMO should have exactly the same molecular weight and molecular weight distribution as the PEEIs of structure **3**; thirdly, the transesterification catalyst and the reaction conditions should be similar. The analytical data of PEE **1** and the analytical data of the PEEIs **2a**–**d**, **3a**–**d** and **4a**–**d** are summarized in Table 1.

The PEEIs **2**–**4** were all prepared by a polycondensation process involving transesterification of the imide monomer **6** with a PTMO diol and an excess of 1,4-dihydroxybutane. The imide monomer **6** was synthesized in a conventional reaction sequence outlined in Scheme 1. The diethyl ester was preferred to the dimethyl ester because of its lower melting point. The polycondensation/transesterification process was catalyzed by titanium tetrabutoxide. The maximum reaction temperature was limited to 250°C quite analogous to the synthesis of PEE **1**. Three different PTMO samples were used having number average molecular weights of 650, 1000 and 2000 Da. For each class of PEEIs (**2**, **3** or **4**) the ratio of imide **6** (+1,4-dihydroxybutane) to PTMO was varied in such a way that the weight percentage of the hard segments changed from 30 to 40, 50 and 60% (see Table 1). This is the typical range of hard segments of commercial TPEs.

An important aspect for the properties of the PEEIs is the problem of macrophase separation during the polycondensation process. Phase separation into a PTMO rich and an imide rich phase has the consequence that the covalent coupling between soft and hard segments remains incomplete and poor mechanical properties are obtained. No macrophase separation was observed when PTMO-650 was used regardless of the hard segment content. In the case of PTMO-1000, a turbidity appeared at the end of polycondensation and the extent of the macrophase separation increased with higher imide/PTMO ratios. In the case of PTMO-2000, the macrophase separation began even after 20–30 min during the transesterification of monomer **6** with 1,4-dihydroxybutane, and poor mechanical properties were the consequence (see below). The fact that the macrophase separation occurred

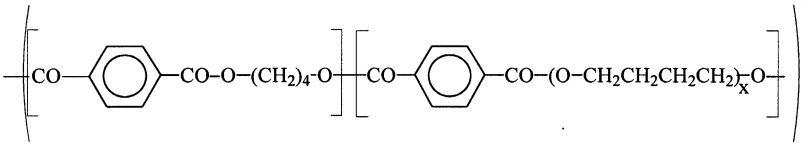

PEE **1** x = (PTMO-1000)

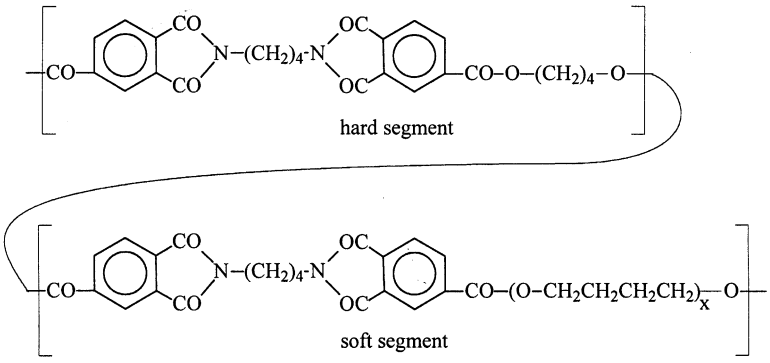

PEEI **2** : x = (PTMO-650)
PEEI **3** : x = (PTMO-1000)
PEEI **4** : x = (PTMO-2000)

Scheme 1.

pretty late in the polycondensation of PTMO-1000 prompted us to study the influence of the polydispersity (PD) on the course of the polycondensation. For this purpose the synthesis of PEEI **3b** was repeated with a PTMO-1000 having a PD of 2.2 instead of 1.9 (characteristic for the first product). With the higher PD no turbidity was observed even at the end of the polycondensation process. The resulting PEEI was listed as **3b′** in Table 1.

The chemical structure of the PEEIs was checked by IR and ^{1}H NMR spectroscopy. A typical IR spectrum is displayed in Fig. 1. The wave numbers of the CO-stretch vibrations of both imide and ester groups were added to the corresponding bands in Fig. 1. Furthermore, the stretch vibration of the ether C–O bonds was identified and characterized by a wave number. The ^{1}H NMR signals were assigned to the individual protons of the **3b** structure in Fig. 2. Both the chemical shifts and the signal intensities agreed with our expectation in all cases. The calculated and experimental weight percentages of the hard segments were in perfect agreement.

Absolute molecular weights were not determined because acidic solvents were required. The inherent viscosities were compared to those of Arnitel® samples provided by DSM. Viscosity values ≥0.60 dl/g were considered to be satisfactory for PEEIs derived from PTMO-650 and viscosities ≥1.0 dl/g were satisfactory for PEEIs of PTMO-1000 or -2000.

3.2. Phase transitions

The melting temperatures (T_ms) of all PEEIs were determined by DSC measurements performed with a heating (and cooling) rate of 20°C/min. The T_ms determined in this way are listed in Table 1. A good reproducibility of these T_ms was found in the second heating trace due to the absence of residual solvent. These measurements revealed three trends, two of which were shown in Fig. 3. Firstly, the T_ms increase with higher fractions of hard segments. At a constant molecular weight of the PTMO segments, a higher fraction of hard segments automatically means longer hard segments which, in turn, will generate larger and more perfect crystallites. Secondly, the T_ms increase with longer PTMO segments. At a constant weight percentage, longer PTMO segments also mean longer hard segments with more perfect crystallites. Furthermore, an increasing lengths of both soft- and hard segments will improve the microphase separation which, in turn, favors the crystallization of the hard segments. Thirdly, a second melting endotherm around 20°C was detectable for all PEEIs of structure **4a–d**. This endotherm represents the melting of the long PTMO chains and is another characteristic indicator of a strong phase separation. The most important and unexpected result was the lack of a crystallization exotherm in the cooling curves of all PEEIs (even at a cooling rate of only −10°C/min). This observation indicates a low rate of crystallization despite the symmetry of imide units in the hard segments,

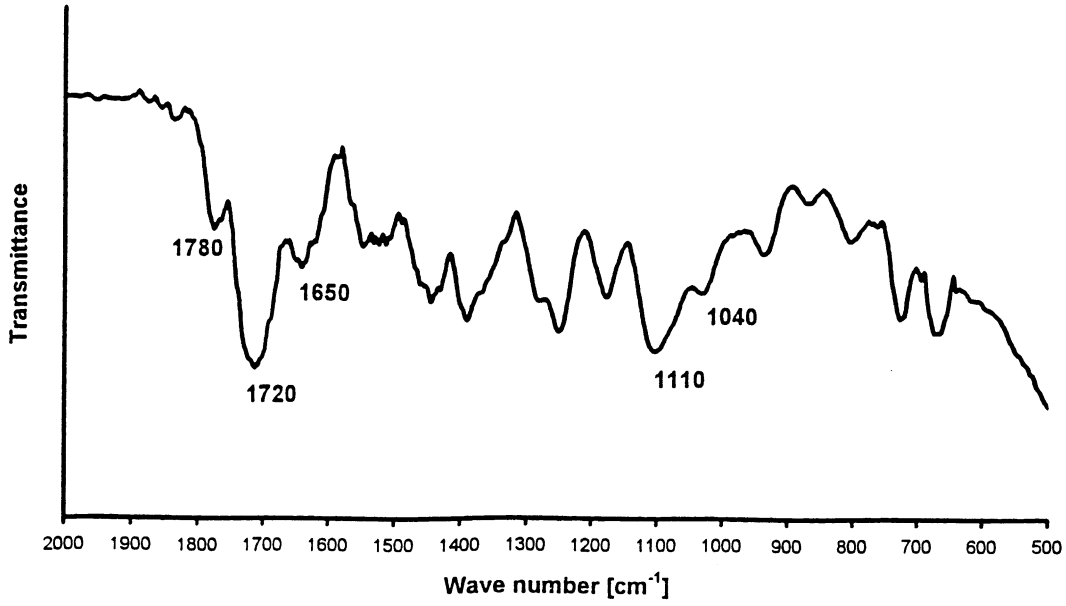

Fig. 1. IR spectrum (KBr pellets) of PEEI **3b′** (PTMO-1000 and 40 wt% hard segments).

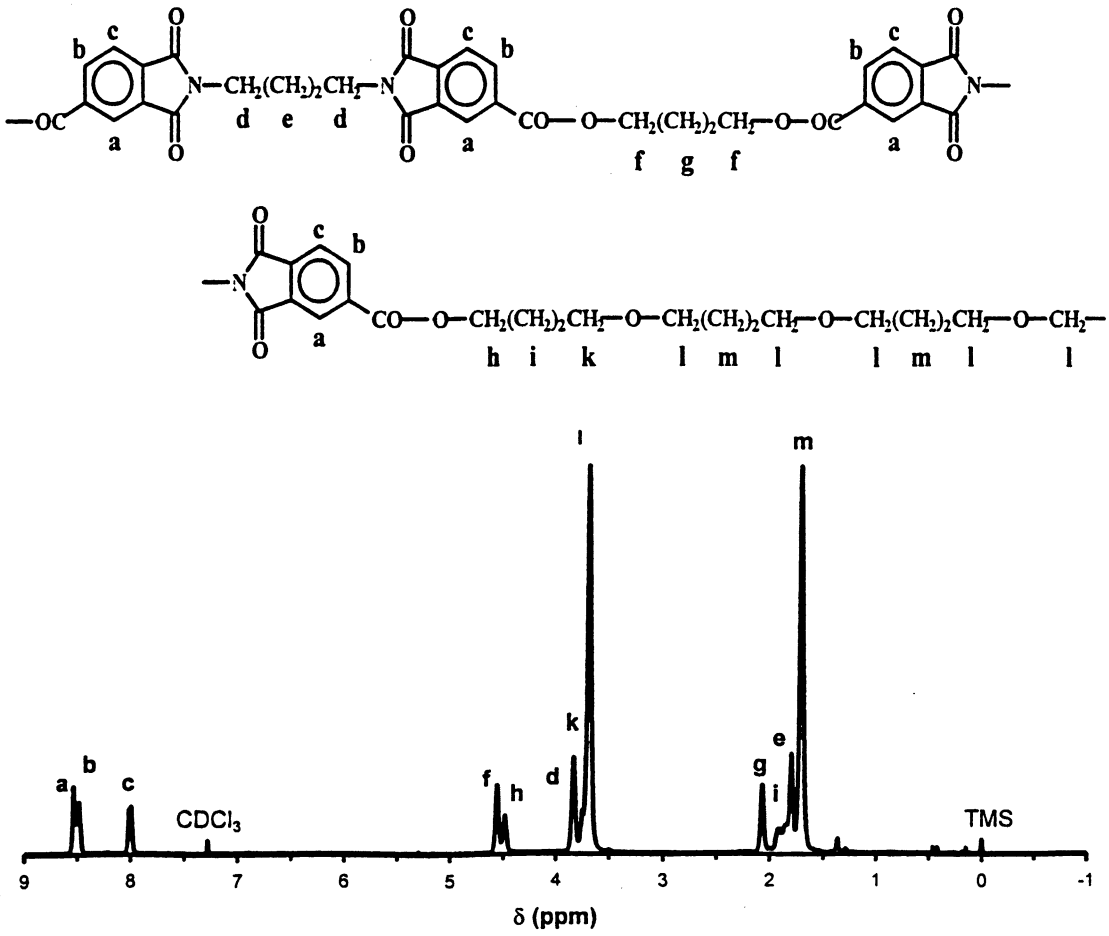

Fig. 2. 400 MHz ^{1}H NMR spectrum of PEEI **3b** (PTMO-1000 and 40 wt% hard segments).

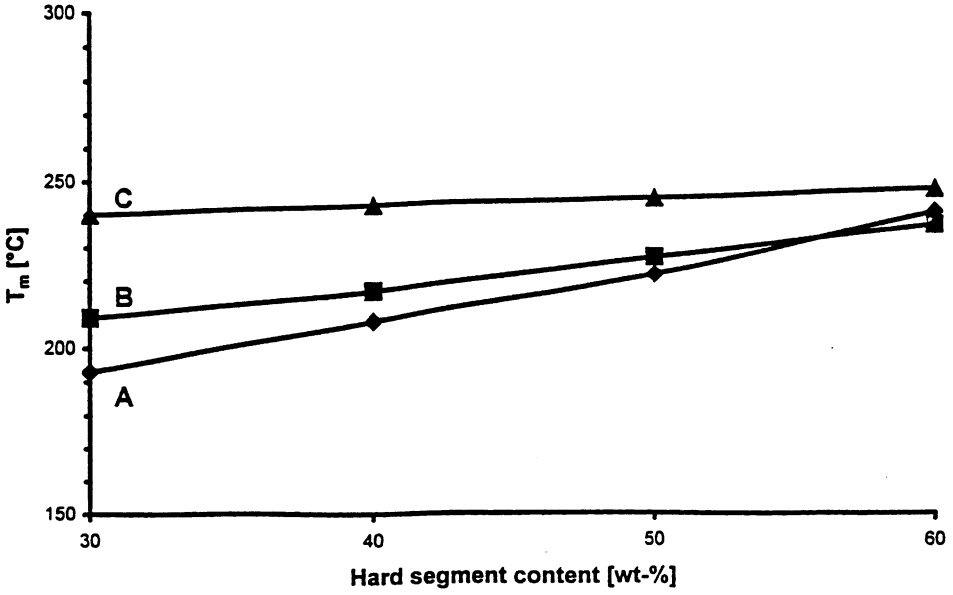

Fig. 3. Dependence of the melting temperatures on the structure of the PEEIs: (A) **2a–d**, (B) **3a–d**, (C) **4a–d**.

despite their planarity and rigidity and despite the flexibility of the butane units. Clearly, the rate of crystallization was too slow for any potential application in injection molding procedures, but it does not hinder applications as films.

For the completion of our study of the crystallinity WAXS powder patterns were recorded which are exemplarily shown in Fig. 4. Without any detailed analysis two conclusions may be drawn. Firstly, the crystallinity was clearly detectable, but the overall degree of crystallinity was low (20–30%) in agreement with a 60% content of amorphous soft segments. Secondly, the chain packing of the hard segment is orthorhombic or monoclinic and certainly not hexagonal.

A few samples were selected for an evaluation of their mechanical properties (see below). From the DMTA measurements, glass-transition temperatures (T_gs) were extracted defined as the maxima of the tan δ curves (Fig. 5). The T_g values fell into a very broad range from −75 to +20°C. The sharp glass transition of **4b** around −75°C agrees with that of the neat PTMO, and thus, is characteristic for an almost perfect phase separation. This observation is in turn in good agreement with the early macrophase

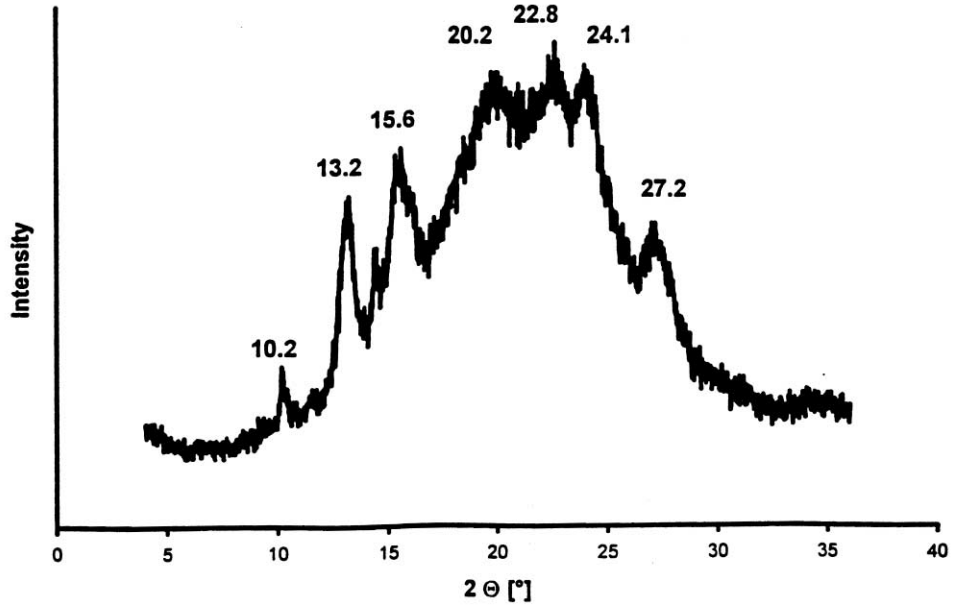

Fig. 4. WAXS powder pattern of PEEI **3b′**.

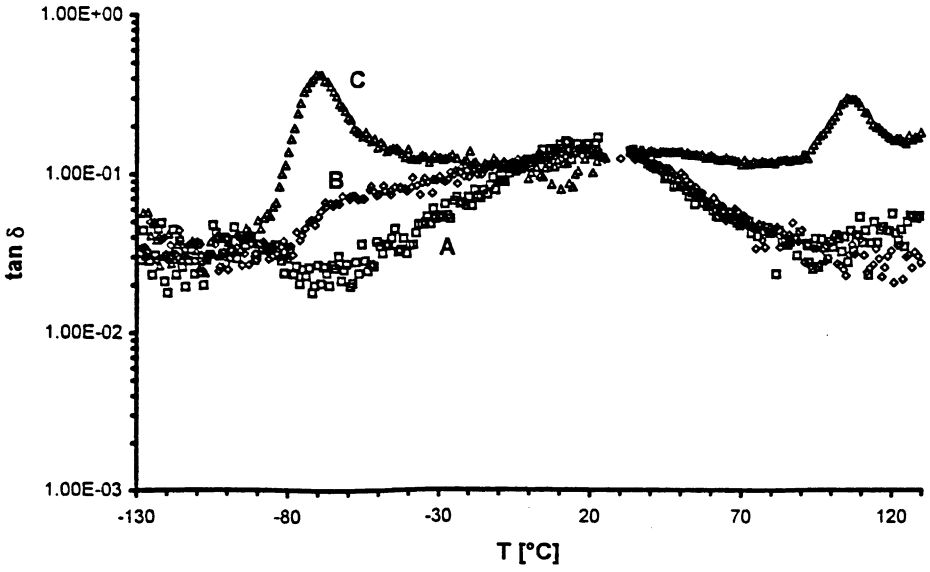

Fig. 5. DMTA measurements (tan δ) of the PEEI **2b**: curve A, PEEI **3b**: curve B, and PEEI **4b**: curve C.

separation during the polycondensation and with the crystallization of the PTMO segments.

In the case of **3b** and **3b′** the glass transition covers a broad range beginning around −70°C and ending with a flat maximum around +20°C (curve B in Fig. 5). These broad glass transitions (including that of **2b**, curve A) were not clearly detectable in the DSC curves. This broad temperature range indicates a poorer phase separation, and raises the question if the amorphous phase is multiphasic. Possibly, a broad variety of domains may coexist ranging from domains rich in long PTMO segments and containing few imide groups up to domains rich in imide units and containing short PTMO segments. In the case of PEEI **2b**, the trend towards an amorphous phase rich in imide units is even more pronounced.

3.3. Mechanical properties

When the DMTA curves shown in Figs. 6 and 7 are analyzed with respect to the storage modulus (E') and to the loss modulus (E''), the following conclusions may be drawn. The storage and loss moduli of **2b** and **3b** show a very broad and flat transition in agreement with the complex amorphous phase discussed above for the glass-transition.

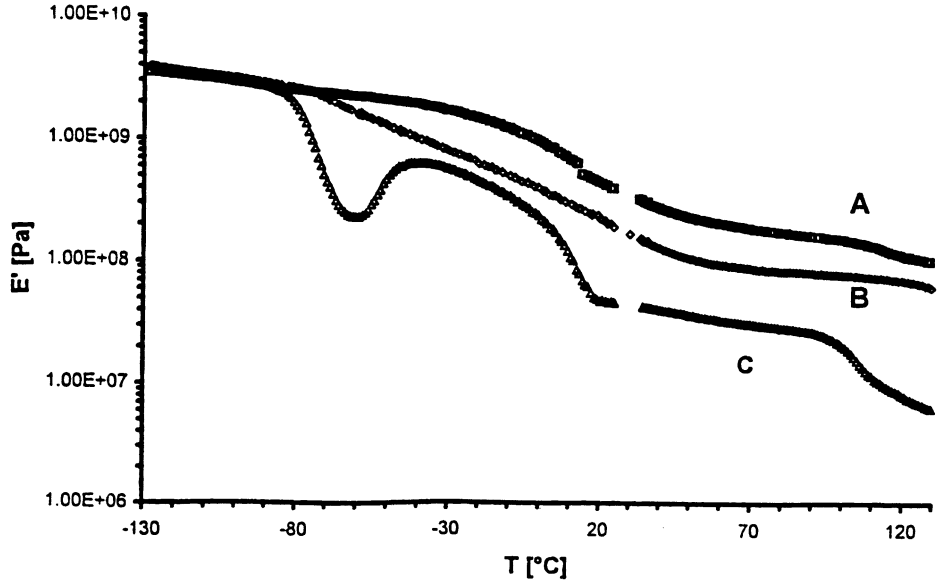

Fig. 6. DMTA measurements (storage modulus) of PEEI **2b**: curve A, PEEI **3b**: curve B, and PEEI **4b**: curve C.

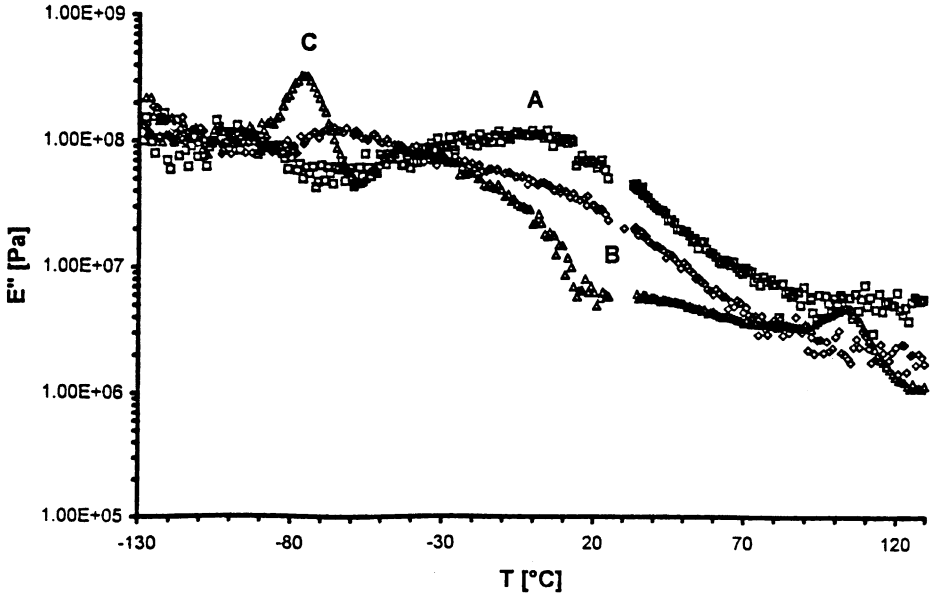

Fig. 7. DMTA measurements (loss modulus) of PEEI **2b**: curve A, PEEI **3b**: curve B, PEEI **4b**: curve C.

In contrast, the good phase separation of PEEI **4b** is reflected in sharp decrease of E' and increase of E'' around −75°C for the glass-transition of the PTMO segments. The following increase of E'' (and increase of E'') results from the crystallization of the PTMO segments. The decrease of E' in the temperature range up to +15°C is a consequence of the melting of the PTMO phase. The additional loss of E'' between 100 and 110°C results most likely from the glass-transition of the hard segment phase, which occurs at 99–100°C in the homopoly(ester-imide) [13]. In the case of the PEEIs studied in this work, this glass-transition is difficult to detect in the DSC measurements.

A comparison with the DMTA measurements of PEE **1** shown in Fig. 8 revealed that both morphology and mechanical properties are somewhat different from all three PEEIs. All three parameters indicate a relatively sharp phase transition at the glass transition temperature around −50°C. Finally the melting of the hard segments causes a second strong change in the E', E'' and tan δ curve.

The stress–strain measurements shown in Fig. 9 revealed the following pattern. The poorest mechanical properties were found for PEEI **4b** (curve D) obviously due to an incomplete coupling of PTMO segments to the hard segments. In contrast, the PEEIs **2b**, **3b** and **3b′** displayed the typical curves expected for true TPEs. In the case of **3b′** both the stress values and the elongation at break were

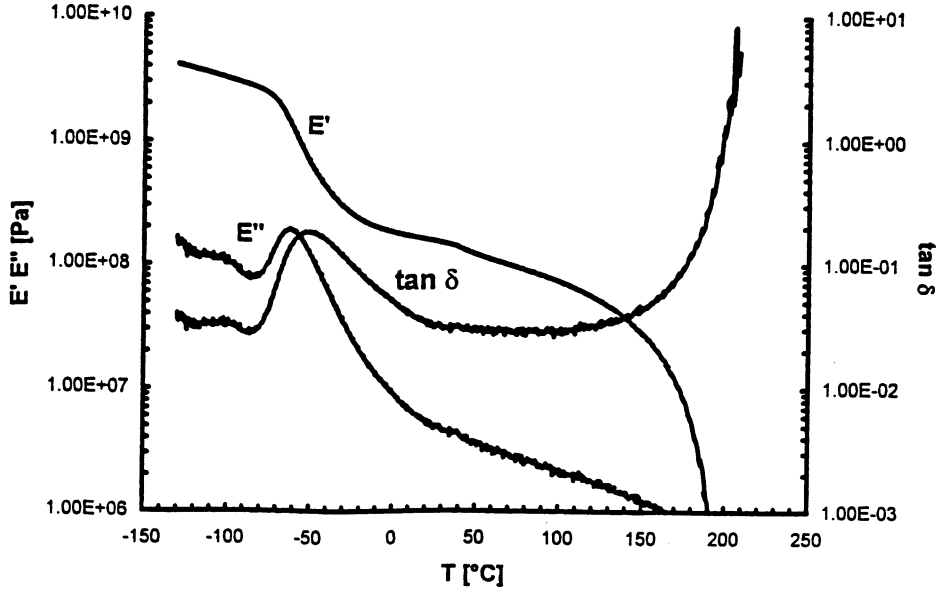

Fig. 8. DMTA measurements of PEE **1**.

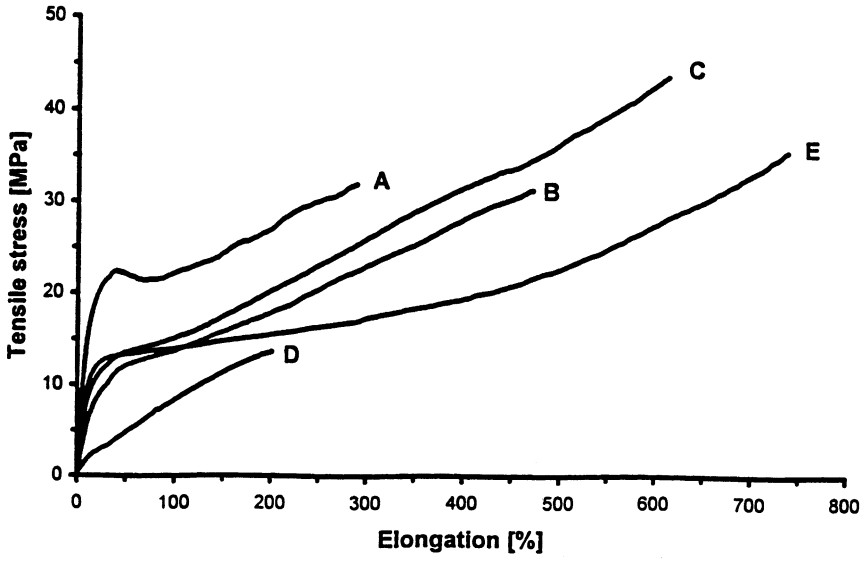

Fig. 9. Stress–strain measurements of: (A) PEEI **2b**, (B) PEEI **3b**, (C) PEEI **3b′** (D) PEEI **4b**, (E) PEE **1**.

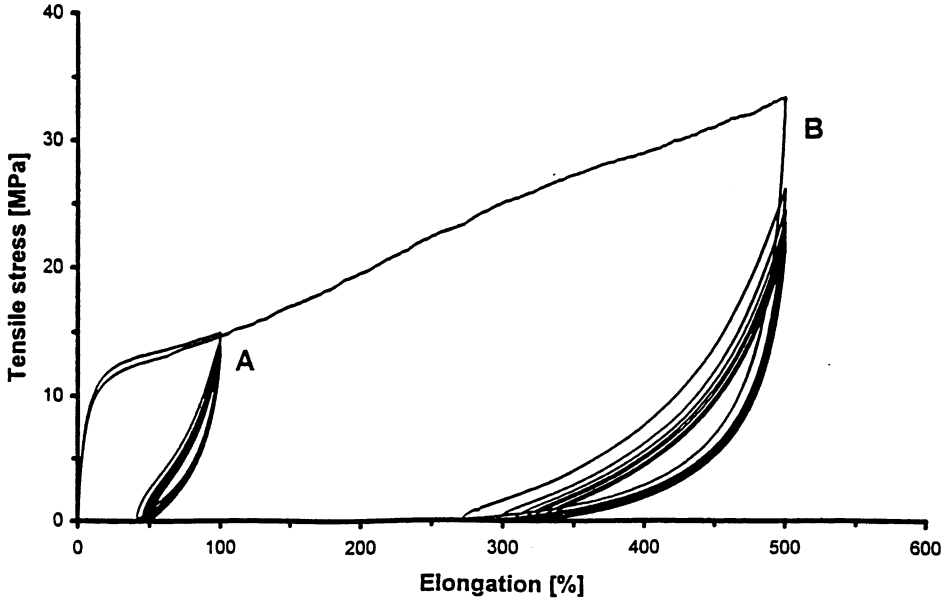

Fig. 10. Hysteresis measurements of PEEI **3b′**.

Table 2
Comparison of phase transitions and mechanical properties of PEEIs **2b**, **3b**, **3b′**, **4b** and PEE **1**

Polymer	T_g[a] (°C)	T_m[b] (°C)	Tensile stress at 100% elongation (MPa)	Elongation at break (%)	Tensile stress at break (MPa)
PEEI **2b**	+20	208	22.2	290	32.0
PEEI **3b**	−60/+20	217	13.7	470	31.0
PEEI **3b′**	−60/+20	219	15.1	614	43.6
PEEI **4b**	−70	243	8.4	200	13.7
PEE **1**	−50	196	14.1	738	35.5

[a] From the tan δ of DMTA measurements.
[b] From the second heating of DSC measurements.

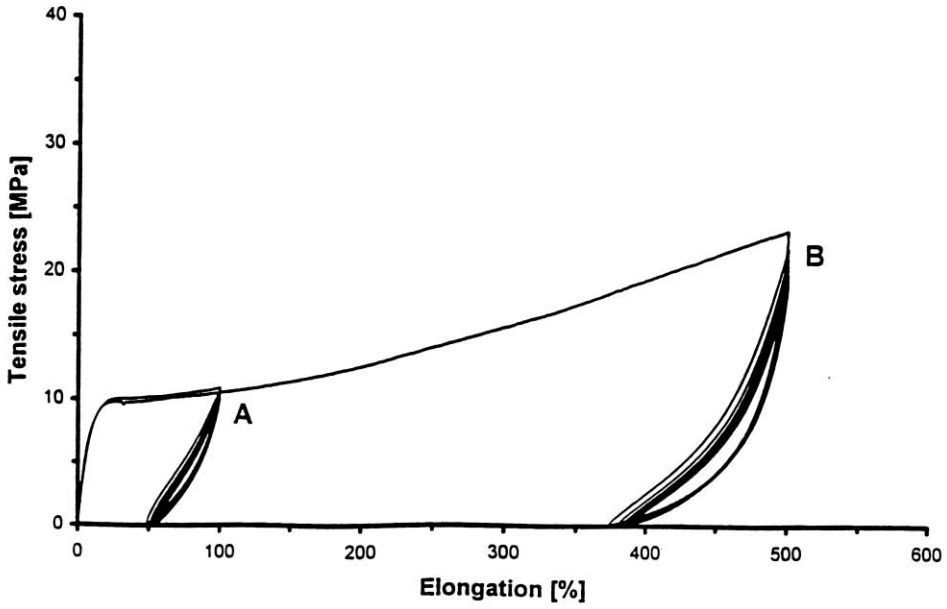

Fig. 11. Hysteresis measurements of PEE **1**.

slightly higher than those of **3b** in agreement with the fact that no macrophase separation had occurred during its synthesis. The stress–strain curve of PEE **1**, which has a composition and PTMO length directly comparable to **3b** and **3b′**, fell exactly in between the curves of these PEEIs. The mechanical data listed in Table 2 also indicate that the elongation at break was somewhat higher than those of both PEEIs. In other words, the stress–strain properties of PEE **1** and **3b** or **3b′** were quite similar, despite different DMTA measurements. As expected, the highest stress values, but the shortest elongation was observed for **2b**, the PEEI containing the shortest PTMO segments.

Finally, hysteresis measurements of the best PEEI (i.e. **3b′**) and of PEE **1** were performed. As illustrated by Figs. 10 and 11 no difference was detectable at 100% initial strain (curve A). However, at 500% initial strain, it became evident that the recovery of PEEI **3b′** was better than that of PEE **1** (curve B). This higher elasticity was not expected considering the poorer microphase separation indicated by the DMTA measurements. In summary, the stress–strain and hysteresis measurements revealed that the PEEIs **3b** and **3b′** possessed better mechanical properties than PEE **1**.

4. Conclusions

New thermoplastic elastomers were prepared from PTMO, 1,4-dihydroxybutane and a bisimide dicarboxylic acid based on 1,4-diaminobutane and trimellitic anhydride. The tendency of phase separation during the polycondensation increased with the lengths of the PTMO diols. With PTMO-2000, an early macrophase separation was observed and poor mechanical properties were obtained, obviously due to incomplete coupling of hard segments and PTMO diols. When a PTMO-1000 of relatively high polydispersity was used, macrophase separation during the synthesis was avoided and good mechanical properties were obtained which can rival with those of a classical TPE based on PBT hard segments. However, all poly(ether-ester-imide)s of this work crystallize slowly and this unexpected property is at least a hindrance for a successful processing by injection molding, but allows their application as films.

References

[1] Coleman D. J Polym Sci 1954;14:15.
[2] Coleman D. Br Pat 682,866, 1952 to ICI plc.
[3] Charch WH, Shrivers JC. Text Res J 1959;29:536.
[4] Shrivers JC. US Pat 3,023,192, 1962 to E.I. DuPont de Nemours.
[5] Nishimura AA, Komogata H. J Macromol Sci, Chem A 1967;1:617.
[6] Witsiepe WK. US Pat 3,651,014, 1972 to E.I. DuPont de Nemours.
[7] Witsiepe WK. US Pat 3,763,109 and 3,755,146, 1973 to E.I. DuPont de Nemours.
[8] Brown M, Witsiepe WK. Rubber Age 1972;104:35.
[9] Adams RK, Hoeschele GK, Witsiepe WK. Thermoplastic polyether ester elastomers. In: Holden G, Legge NR, Quirk R, Schroeder HE, editors. Thermoplastic elastomers, 2nd ed. New York: Hanser, 1996. Chap. 8.
[10] Sheridan ThW. Copolyester thermoplastic elastomers. In: Walker BM, Rader CP, editors. Handbook of thermoplastic elastomers, 2nd ed. New York: Van Nostrand-Rheinhold, 1989. Chap. 6.
[11] van Berkel RWM, Borggreve RJM, van der Sluijs CL, Werumeus-Buning GHW. Poly-ester-based thermoplastic elastomers. In: Olabisi O, editor. Handbook of thermoplastics. New York: Marcel Dekker, 1997. Chap. 17.
[12] Kricheldorf HR, Pakull R. Macromolecules 1988;21:551.
[13] Schmidt B, Koning CE, Werumeus-Buning GHW, Kricheldorf HR. J Mater Sci, Pure Appl Chem 1997;A34:759.